Original Research Article

Human and Experimental Toxicology
Volume 42: 1–10

DOI: 10.1177/09603271221149663
journals.sagepub.com/home/het

Mitochondrial ROS induced by ML385, an Nrf2 inhibitor aggravates the ferroptosis induced by RSL3 in human lung epithelial BEAS-2B cells

Indra Putra Taufani[1,2,*], Jiro Hasegawa Situmorang[3,4,*], Rifki Febriansah[5], Sri Tasminatun[5], Sunarno Sunarno[4], Liang-Yo Yang[6,7], Yi-Ting Chiang[8] and Chih-Yang Huang[3,9,10,11,12]

Abstract

Ferroptosis is a new type of cell death marked by iron and lipid ROS accumulation. GPX4 is one of the glutathione peroxidases known to regulate ferroptosis tightly. On the other hand, Nrf2 also plays a vital role in ferroptosis as it targets genes related to oxidant defense. Herein, we employed beas-2 human epithelial cells treated with a low concentration of RSL3 to induce ferroptosis. To study the protective role of Nrf2, we used ML385 as its specific inhibitor. A combination of ML385 and a low concentration of RSL3 synergistically induced more toxicity to RSL3. Furthermore, we found that mitochondrial ROS is elevated in ML385 and RSL3 combination group. In addition, Mito TEMPOL application successfully prevents the upregulation of mitochondrial ROS, lipid ROS, reduces the toxicity of RSL3, restores the antioxidant capacity of the cells, and mitochondrial functions reflected by mitochondrial membrane potential and mitochondrial oxidative phosphorylation system (OXPHOS) expression. Altogether, our study demonstrated that Nrf2 inhibition by ML385

[1]Graduate Institute of Pharmacy, China Medical University, Taichung, Taiwan
[2]Department of Pharmacist Profession Education, Faculty of Medicine and Health Sciences, Universitas Muhammadiyah Yogyakarta, Yogyakarta, Indonesia
[3]Cardiovascular and Mitochondrial Related Disease Research Center, Buddhist Tzu Chi General Hospital, Buddhist Tzu Chi Medical Foundation, Hualien, Taiwan
[4]Center for Biomedical Research, National Research and Innovation Agency (BRIN), Cibinong, Indonesia
[5]School of Pharmacy, Faculty of Medicine and Health Sciences, Universitas Muhammadiyah Yogyakarta, Yogyakarta, Indonesia
[6]Department of Physiology, School of Medicine, College of Medicine, China Medical University, Taichung, Taiwan
[7]Laboratory for Neural Repair, China Medical UniversityHospital, Taichung, Taiwan
[8]School of Pharmacy, China Medical University, Taichung, Taiwan
[9]Graduate Institute of Medical Science, China Medical University, Taichung, Taiwan
[10]Department of Medical Research, China Medical University Hospital, China Medical University, Taichung, Taiwan
[11]Department of Biotechnology, Asia University, Taichung, Taiwan
[12]Center of General Education, Buddhist Tzu Chi Medical Foundation, Tzu Chi University of Science and Technology, Hualien, Taiwan

*Both authors contributed equally to this study.

Corresponding authors:
C-Y Huang, Cardiovascular and Mitochondrial Related Disease Research Center, Hualien Tzu Chi Hospital, Buddhist Tzu Chi Medical Foundation. Tzu Chi University of Science and Technology, No. 707, Sec. 3, Zhongyang Rd, Hualien 970, Taiwan.
Email: cyhuang@mail.cmu.edu.tw

Y-T Chiang, School of Pharmacy, China Medical University, No. 91, Xueshi Rd, North District, Taichung 404, Taiwan.
Email: ytchiang@mail.cmu.edu.tw

L-Y Yang, Department of Physiology, School of Medicine, College of Medicine, China Medical University, Laboratory for Neural Repair, China Medical University Hospital, No. 91, Xueshi Rd, North District, Taichung 404, Taiwan.
Email: yangly@mail.cmu.edu.tw

induces more toxicity when combined with RSL3 through the elevation of mitochondrial ROS and disruption of mitochondrial function.

Keywords
Ferroptosis, Nrf2 inhibition, mitochondrial ROS, RSL3, Mito TEMPOL, GPX4, OXPHOS

Introduction

A new form of cell death, ferroptosis, was discovered just a decade ago. This new type of cell death is marked by the accumulation of lipid peroxides and intracellular labile iron.[1] Since then, many kinds of diseases, such as diabetes, neurological disorders, fatty liver, cancer, and lung diseases, have been linked to this type of cell death.[2,3] One of the critical proteins that tightly regulates ferroptosis is glutathione peroxidase 4 (GPX4), which belongs to the glutathione peroxidase family. It mainly helps to clear lipid peroxides to protect the cells from oxidative stress by catalyzing lipid peroxides into nontoxic lipid alcohols.[4] One of the potent inhibitors of GPX4 is RAS selective lethal 3 (RSL3). Studies have shown that RSL3 drives cells into ferroptosis cell death by binding to GPX4 and inactivates it.[5] Although GPX4 plays a crucial role in regulating ferroptosis, another protein which is Nrf2, also plays an essential role in regulating ferroptosis since GPX4 is a downstream target of Nrf2. Moreover, Nrf2 is critical in regulating iron homeostasis by controlling genes involved in heme synthesis, hemoglobin catabolism, iron storage, and iron export.[6]

Mitochondria are organelles that regulate energy generation, which fuels cell metabolisms. As a byproduct of electron chain activity, reactive oxygen species (ROS) are generated in mitochondria. Interestingly, excessive mitochondrial ROS is an initiator in triggering cell death. On the other hand, studies show mitochondria also play an essential role as a defense factor against ferroptosis through their own GPX4.[7]

In this study, we used ML385, a small molecule of Nrf2 inhibitor that binds to the Neh1 domain of Nrf2,[8] to investigate the role of Nrf2 in protecting the beas-2b lung epithelial cells from ferroptosis induced by RSL3. More importantly, herein, we showed that mitochondrial ROS plays a crucial role in aggravating the toxicity of RSL3.

Materials and methods

Materials

Beas-2b human epithelial cell line was purchased from ATCC (Manassas, VA, USA). Dulbecco's Modified Eagle's Medium: Nutrient Mixture F-12 (DMEM/F-12), phosphate buffered saline (PBS), and 100X penicillin-streptomycin (10,000 U/mL) were purchased from Life Technologies Corporation (Grand Island, NY, USA). Fetal bovine serum (FBS) was purchased from Hyclone (Logan, UT, USA). BioTrace™ nitrocellulose transfer membrane was purchased from Pall (Port Washington, NY, USA). RSL3 (19288) and ML385 (21114) were purchased from Cayman (Ann Arbor, MI, USA). Mito TEMPOL (ab144644) was purchased from Abcam (Waltham, MA, USA). CCK-8 cell counting kit was purchased from Vazyme (Nanjing, China). MitoSOX™, BODIPY™ 581/591 C11, and MitoProbe™ JC-1 Assay Kit were purchased from Invitrogen (Waltham, MA, USA). Bradford protein assay kit was purchased from Bio-Rad (Hercules, CA, USA). Antibodies against GPX4 (#52455), TfR1 (#13113), were purchased from Cell Signaling Technology (Danvers, MA, USA). Antibody against Nrf2 (A1244) was purchased from Abclonal Technology (Woburn, MA, USA). Antibody against total OXPHOS Rodent WB Cocktail (ab110413) was purchased from Abcam (Waltham, MA, USA). Antibodies against GAPDH (sc-32233), mouse and rabbit secondary antibodies were purchased from Santa Cruz Biotechnology (Dallas, TX, USA). Immobilon Western Chemiluminescent HRP Substrate was purchased from Millipore (Burlington, MA, USA).

Mito TEMPOL, ML385, and RSL3 preparation

Mito TEMPOL was dissolved in Milli-Q water. ML385 or RSL3 was dissolved in DMSO. Upon received, all the chemicals were prepared to make a 5 mM final concentration. All the solutions were aliquoted and kept in tightly sealed dark tube at −80°C.

Culture of beas-2b cells

Beas-2b was maintained in DMEM/F-12 supplemented with 10% FBS and 1X penicillin-streptomycin at 37°C in a humidified 5% CO_2 incubator. Once the cells reached around 80% confluence, they were seeded in 6-well or 12-well culture plates for experiments. Before RSL3, ML385, and Mito TEMPOL treatments, the growth media was replaced with DMEM/F-12 without serum to make the cells quiescent for overnight.

Viability assay

Beas-2b cells were cultured in 12-well plates, after they reached 80% confluence, the growth media was replaced with DMEM/F12 without serum and the cells were

incubated at 37°C for overnight before further treatment. After treatment, the viability of the cells was measured by using CCK-8 assay kit. Briefly, CCK-8 solution was mixed with the growth media (20 µL/mL) and 500 µL was added to each well and incubated for 2 h at 37°C. The absorbance at 460 nm was measured with Epoch™ BioTek Instruments microplate spectrophotometer.

Mitochondrial ROS detection

The MitoSOX molecular probe was used to detect mitochondrial ROS generation in beas-2b cells. The protocol was similar to previous studies[9,10] in which we used low concentration of MitoSOX diluted in DMEM/F12 without serum (1 µM) instead of using 5 µM to avoid non-specific staining. After treatment with RSL3 with or without ML385 or Mito TEMPOL, the media was removed, and the cells were washed with PBS one time. Then, the MitoSOX solution was added, and the cells were incubated for 20 min in a 37°C incubator. After incubation, the MitoSOX solution was removed, and the cells were trypsinized and subjected to flow cytometry analysis with the Ex/Em wavelength in the range of 510/580 nm.

Lipid ROS detection

An explanation of the detailed procedure has been provided in a previous study.[11] The BODIPY^{TM} 581/591 C11 probe was used to detect lipid ROS generation in beas-2b cells. The BODIPY^{TM} 581/591 C11 was diluted in DMSO to make 1.5 mM stock solution. After treatment, the media was removed, and replaced with working solution of BODIPY^{TM} 581/591 C11 diluted in growth media for 1.25 µM incubated for 30 min in a humidified 37°C incubator. After incubation, the cells were harvested and subjected to flow cytometry analysis.

Analysis of mitochondrial membrane potential

Detail procedure has been described in the previous study.[12] Briefly, for the assessment of mitochondrial membrane potential, 5′,6′-tetrachloro-1,1′,3,3′-tetraethyl benzimidazolyl carbocyanine iodide dye (JC-1) was used. We prepared the JC-1 working solution by mixing 200X of JC-1 stock solution with growth media to obtain a final concentration of 2.5 mg/mL. Then, the cells were incubated at 37°C for 30 min with the working solution. JC-1 aggregates and monomer were analyzed by flow cytometry using wavelengths of 520/590 nm and 490/530 nm, respectively.

Western blot analysis

The protocol used was similar to previous studies.[13,14] Following treatment, the cells were harvested. The media was removed and the cells were washed with PBS. The mixture of 2X Laemmli buffer and 2X RIPA buffer in 1:1 ratio was added to collect the cells. The total protein was measured using Bradford assay kit. Around 20–30 µg of total protein were separated in 10% SDS-PAGE gel for 100 min and 90 V conditions, and then transferred to a nitrocellulose membrane. The membrane was cut according to the desired protein size, and then incubated in primary antibody (1:1000) diluted in 5% BSA at 4°C for overnight. The following day, the primary antibody solution was removed, and the membrane was washed thrice for 5 min each with tris buffered saline containing 1% Tween 20. Thereafter, the membrane was incubated with appropriate secondary antibody (1:5000) diluted in 5% BSA at RT for 1 h. Finally, chemiluminescent substrate was used to visualize the proteins. The signal was captured by using UVP ChemStudio Plus touch (Analytik Jena; Jena, Germany). The images were quantified using ImageJ (NIH).

Immunofluorescence staining

The protocol for immunofluorescence staining has been described in detail in the previous study.[15] Briefly, the cells were fixed with 4% paraformaldehyde after treatment for 5 min, followed by washing with PBS thrice for few seconds. Next, 1% BSA was added to block the unspecific binding of antibodies for 30-min at RT. After blocking, the cells were incubated with primary antibody overnight at 4°C. The following day, the primary antibody solution was removed, and the cells were washed with PBS thrice. Finally, a secondary antibody was added for one hour at RT. The cells were mounted with DAPI solution and covered with coverslips. The images were taken using fluorescence microscopy (Olympus), with the excitation and emission wavelength in the range of 358/461 for DAPI and 590/617 nm for GPX4 and TfR1.

Statistical analysis

Data were shown as mean ± S.E.M. and were plotted and analyzed statistically with GraphPad Prism version 7.0.0. p value of $<.05$ was considered statistically significant.

Results

Nrf2 inhibition by ML385 worsen the ferroptosis induced by RSL3

Nrf2 protects the cells from ferroptosis through its tarWget gene, where it prevents lipid peroxides and intracellular iron accumulation.[16] In Figures 1(a) and (b), Nrf2 inhibition by various concentrations of ML385 treatment for 4-h and 8-h showed little effect on beas-2b cell viability. In Figures 1(c) and (d), treatment with RSL3 for 4-h and 8-h concentration-dependently reduced cell viability where the maximum

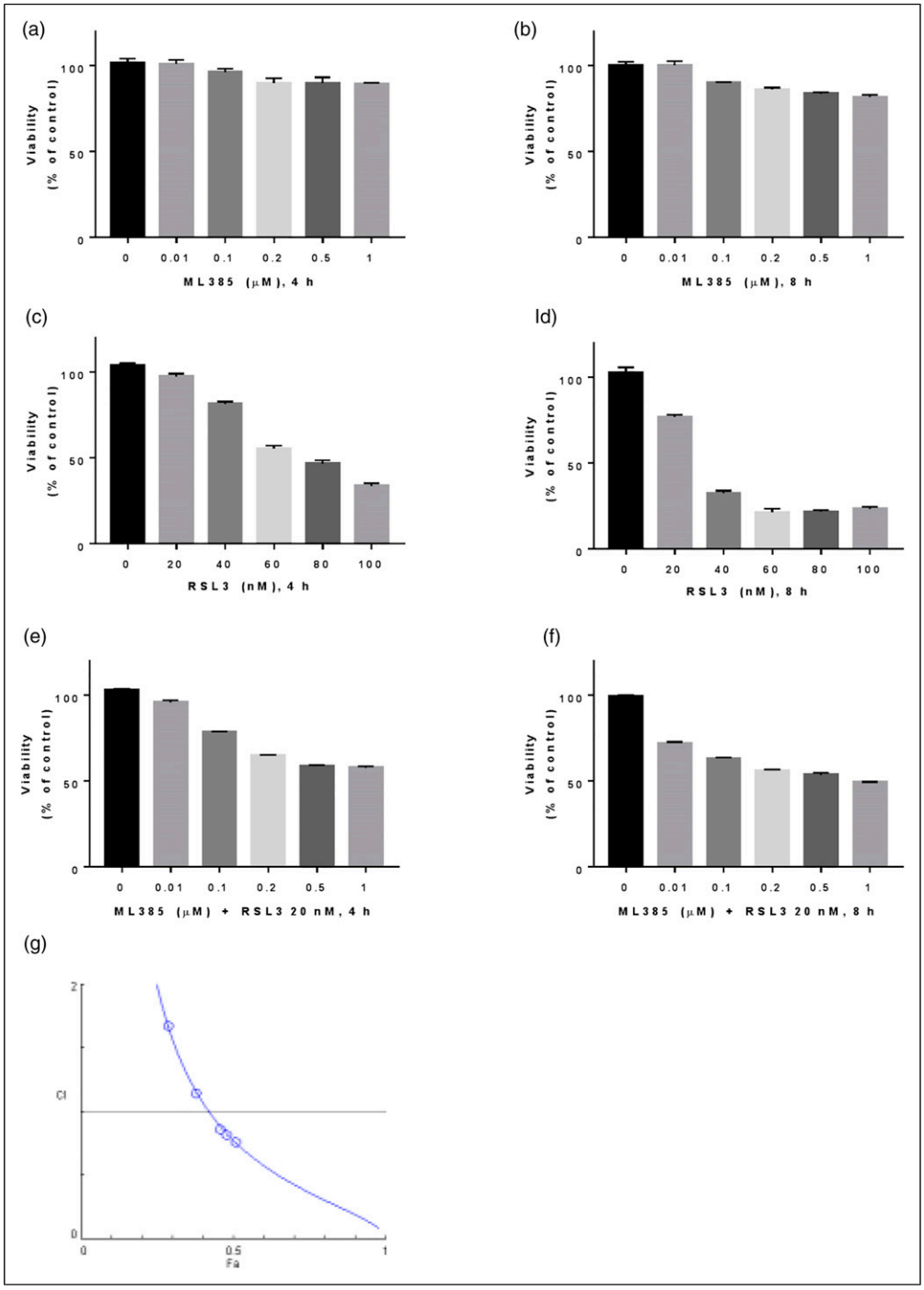

Figure 1. Nrf2 inhibition by ML385 worsen the ferroptosis induced by RSL3. Beas-2b cells were cultured in serum-free medium for 12 h and treated with various concentrations of ML385 for 4-h (a) and 8-h (b). Challenge with RSL3 for 4-h (c) and 8-h (d) concentration-dependently decreases cell viability of Bease-2b cells. Combination of various concentrations of ML385 and 20 nM of RSL3 for 4-h (e) and 8-h (f) worsen the reduction of the cell viability. The cell viability was measured by CCK-8 assay. Fa-CI plot (g) shows synergistic effect of ML385 and RSL3 combination. Data are expressed as mean ± SEM.

response was achieved by 60 nM of RSL3 for 8-h. To know the effect of Nrf2 inhibition on ferroptosis, we pretreated the cells with various concentrations of ML385 for 1-h before treatment with 20 nM of RSL3 for 4-h (Figure 1(e)) and 8-h (Figure 1(f)). Our results showed the maximum effect could be seen at 0.5 μM of ML385. Further, we made the Fa-CI plot using CompuSyn software (Figure 1(g)) to assess the synergism between ML385 and RSL3.

Nrf2 inhibition by ML385 worsen the reduction of antioxidant capacity induced by RSL3

GPX4 is important regulator of ferroptosis whereas Nrf2 is a master regulator of many antioxidant genes that involve in ferroptosis including GPX4.[16,17] In this experiment, we showed that Nrf2 inhibition by ML385 worsen the ferroptosis induced by RSL3 (Figure 2(a)). In addition, we showed that combination of ML385 and RSL3 treatment magnified the downregulation of Nrf2 (Figure 2(b)) and GPX4 (Figure 2(c)) protein expression.

Elevation of mitochondrial ROS level induced by ML385 contributes to the increased toxicity by RSL3

Previous studies showed that ferroptosis induced by RSL3 through GPX4 inhibition does not involve other than lipid ROS.[18] Consistently, our data showed that mitochondrial ROS level is relatively stable at 8-h post RSL3 treatment. Surprisingly, mitochondrial ROS level is increased concentration-dependently if the cells are pretreated with 0.5 μM of ML385, indicating the role of Nrf2 in maintaining mitochondrial ROS level. Treatment with 5 μM Mito TEMPOL, a specific mitochondrial ROS scavenger, as expected, prevented the upregulation of mitochondrial ROS (Figure 3(a)). We also assessed the viability of beas-2b cells where the combination of ML385 and RSL3 exacerbated the viability of the cells. In contrast, Mito TEMPOL treatment rescued the worsening effect of ML385 (Figure 3(c)).

Mito TEMPOL improves antioxidant capacity and prevents ferroptosis marker upregulation

In this experiment, we are interested in checking GPX4, Nrf2, and TfR1 protein expression after Mito TEMPOL

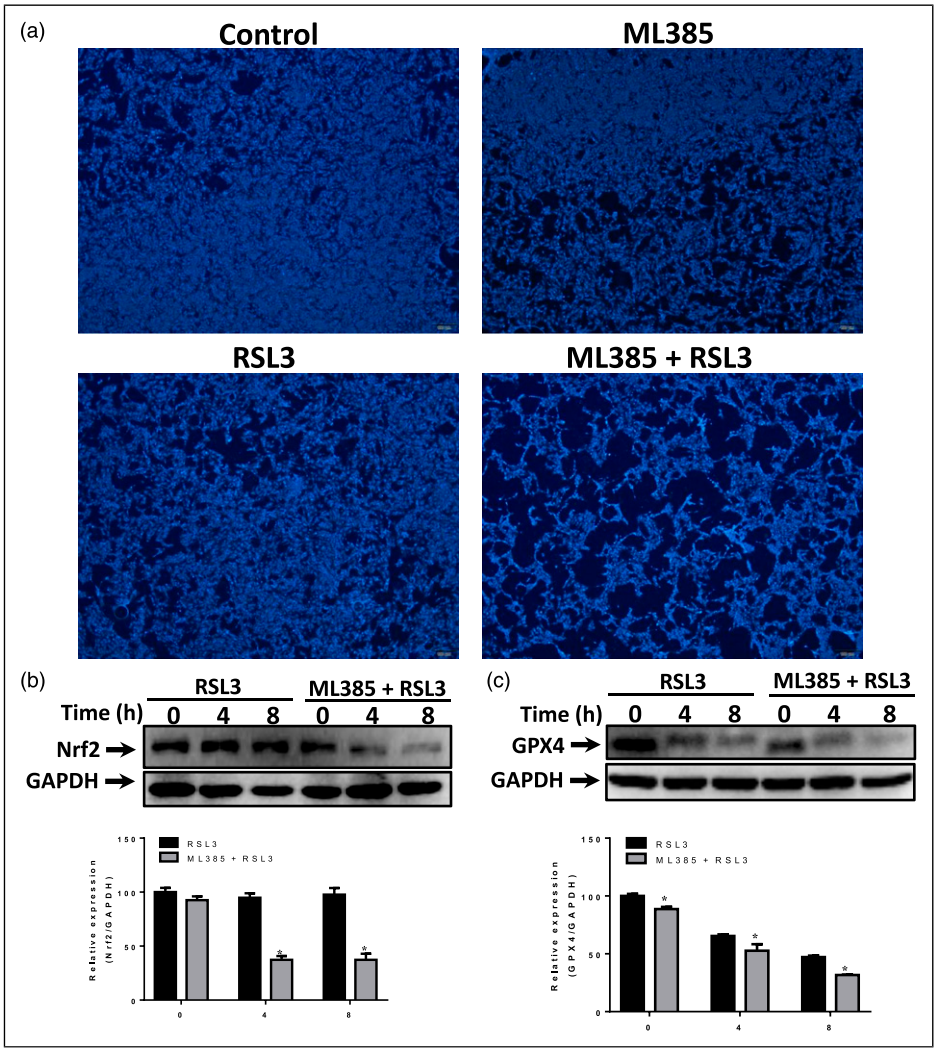

Figure 2. Nrf2 inhibition by ML385 worsen the reduction of antioxidant capacity induced by RSL3. Beas-2b cells were cultured in serum-free medium for 12 h before treated with RSL3 (20 nM), ML385 (0.5 μM), and their combination for 8-h (a). The cells were stained by DAPI to mark nuclei. Western blot was used to measure Nrf2 (b) and GPX4 (c) after treatment with RSL3 alone or its combination with ML385. Data are expressed as mean ± SEM *p-value<0.05 considered as a significant difference compared with control.

treatment. Our data showed that Mito TEMPOL prevented the downregulation of GPX4 after ML385 and RSL3 combination treatment (Figure 4(a)). Previous studies show that TfR1 is a specific biomarker for ferroptosis.[19,20] Hence, we want to see whether Mito TEMPOL treatment can affect TfR1 expression. As expected, Mito TEMPOL also inhibits the upregulation of TfR1 in beas-2b cells.

Mito TEMPOL prevents lipid ROS upregulation and mitochondrial dysfunction

Ferroptosis is mainly characterized by an increase in lipid ROS. As expected, the flow cytometry analysis (Figure 5(a)) showed that 20 nM of RSL3 treatment for 8 h increased lipid ROS in the cells. Interestingly, ML385 did not produce higher lipid ROS when combined with RSL3. On

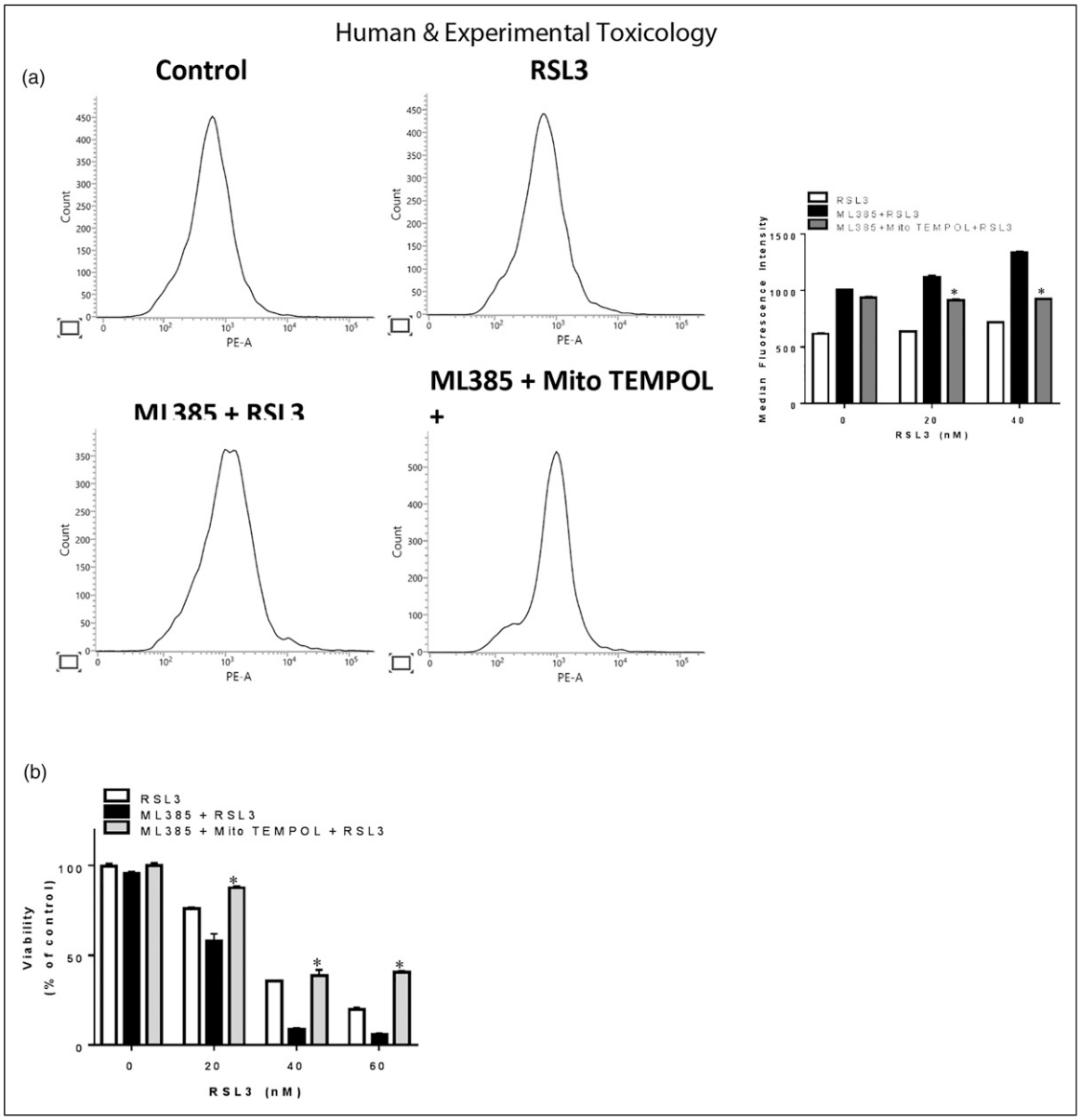

Figure 3. Elevation of mitochondrial ROS level induced by ML385 contributes to the increased toxicity by RSL3. Beas-2b cells were cultured in serum-free medium for 12 h. Before RSL3 (20 nM) treatment for 8-h, the cells were pretreated with ML385 (0.5 μM) for 1-h followed by Mito TEMPOL (5 μM) for 30-minutes. To measure mitochondrial ROS level, MitoSOX staining were performed. The fluorescence intensity was measured by flow cytometry. The cell viability was measured by CCK-8 assay. Mito TEMPOL treatment prevented the elevation of mitochondrial ROS (a) and the reduction of cell viability (b) induced by ML385 and RSL3 combination. Data are expressed as mean ± SEM. *p-value<.05 considered as a significant difference compared with ML385+RSL3.

the other hand, Mito TEMPOL treatment restored the lipid ROS level comparable to control. To evaluate mitochondrial function, we assessed mitochondrial membrane potential by using JC-1 staining. Our results showed that ML385 exacerbated the reduction in the dimer/monomer (red/green) ratio (Figure 5(b)). Mito TEMPOL pretreatment restored membrane potential after RSL3 20nM treatment. As mitochondrial OXPHOS complex activity is critical for mitochondrial respiration, we analyzed them using Western blot. A combination of ML385 and RSL3 produced significant reductions in complex II and IV (Figure 5(c)).

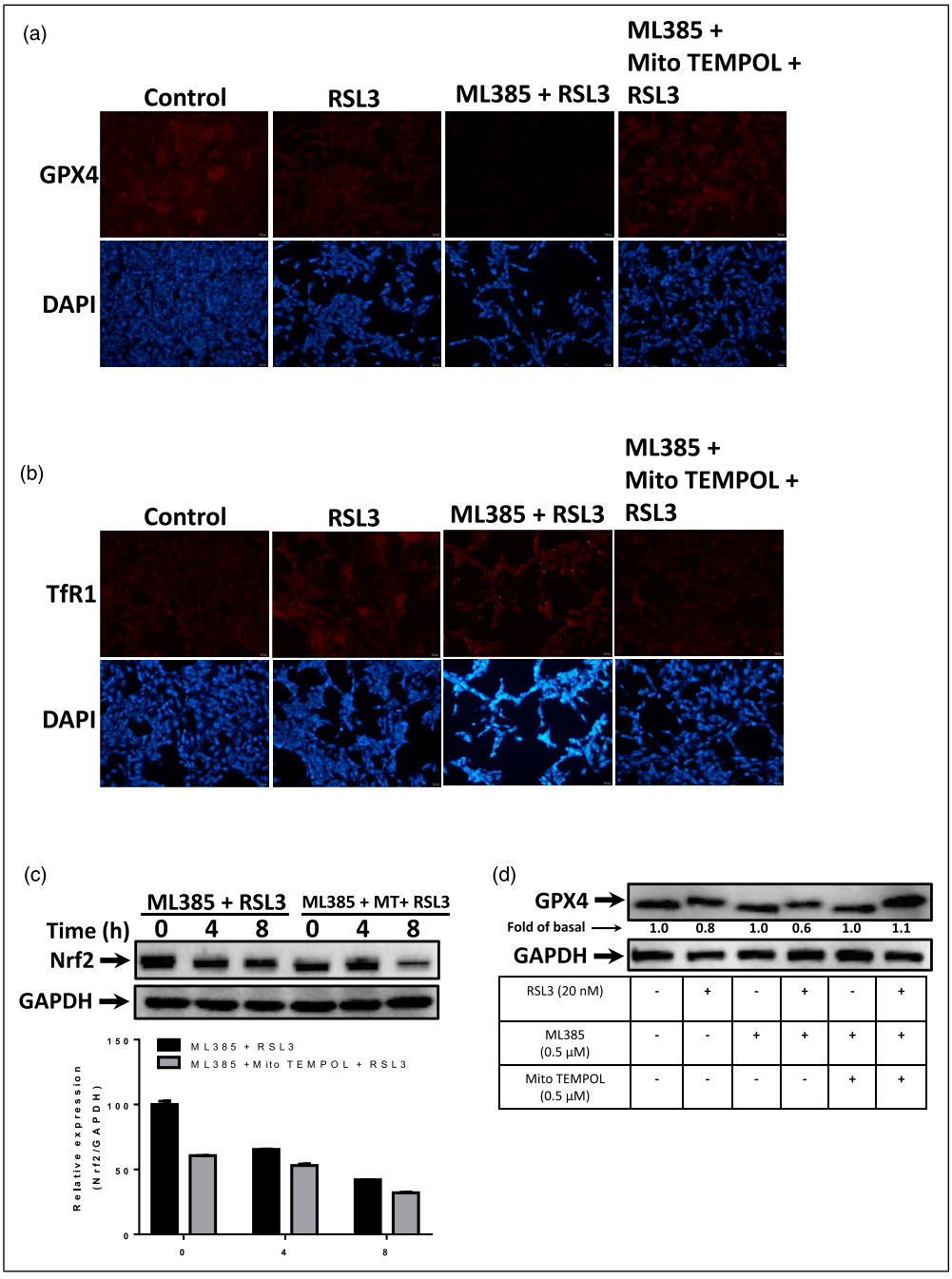

Figure 4. Mito TEMPOL improves antioxidant capacity and prevents ferroptosis marker upregulation. Beas-2b cells were cultured in serum-free medium for 12 h before treated with RSL3 (20 nM), ML385 (0.5 μM), and Mito TEMPOL (5 μM) for 8-h. After treatment, GPX4 (a) and (b) TfR1 expression were assessed by immunofluorescence staining with respective antibody. Western blot was used to measure Nrf2 expression (c) after indicated treatment and GPX4 expression (d) after 2-h treatment.

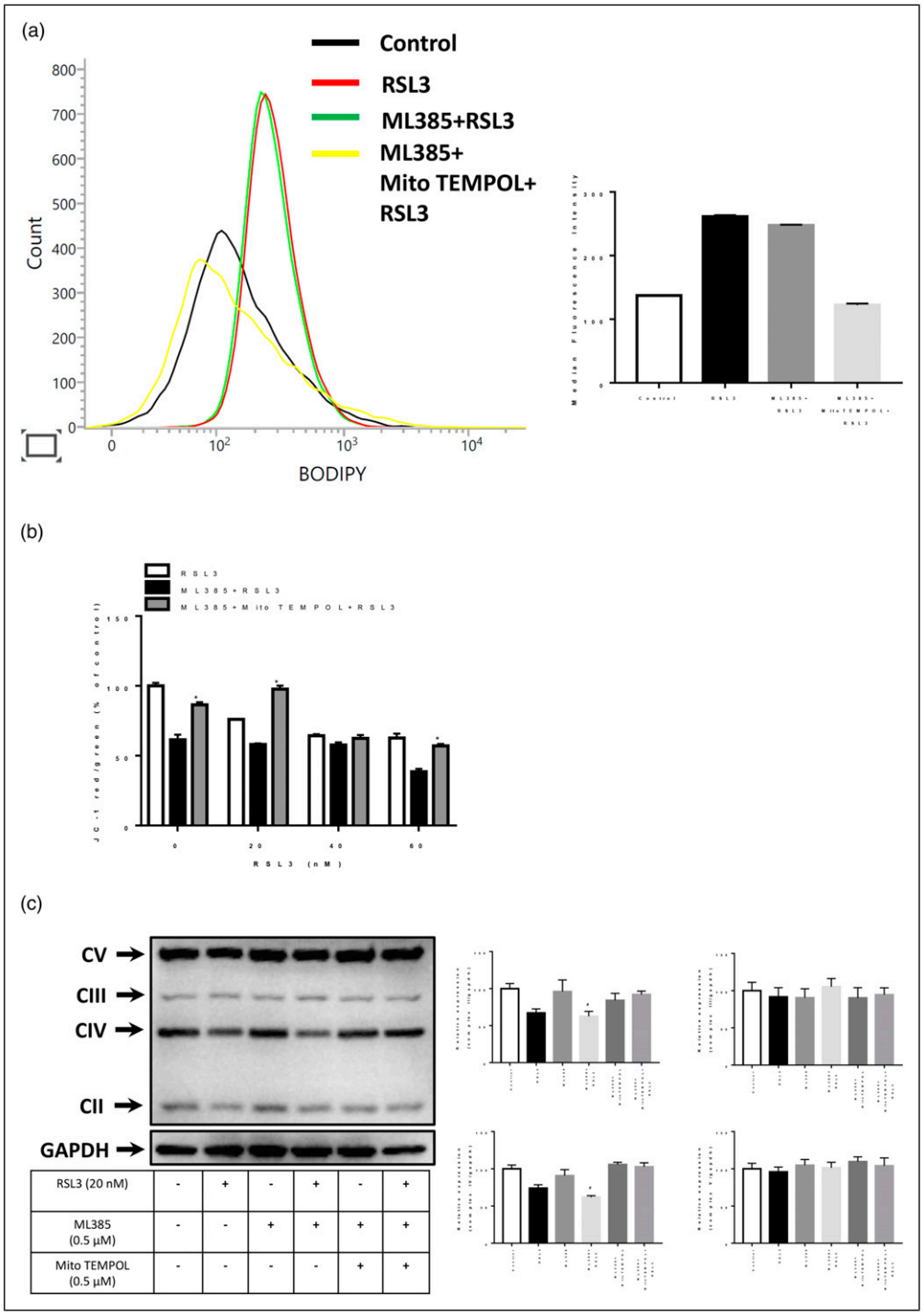

Figure 5. Mito TEMPOL prevents lipid ROS upregulation and mitochondrial dysfunction. Beas-2b cells were cultured in serum-free medium for 12 h before treated with RSL3 (20 nM), ML385 (0.5 μM), and Mito TEMPOL (5 μM) for 8-h. After treatment, lipid ROS (a), and mitochondrial membrane potential (b) were assessed by flow cytometry. Mitochondrial OXPHOS complexes (c) were assessed by Western blot. Data are expressed as mean ± SEM *p-value<.05 considered as a significant difference compared with ML385+RSL3. #p-value<.05 considered as a significant difference compared with control.

Discussion

In the last decade, the new type of cell death, ferroptosis, has become a hot topic as it links to various diseases ranging from cancers to metabolic disorders.[21] This study uses human lung epithelial cells to model ferroptosis in vitro. To our knowledge, we are the first to prove that mitochondrial ROS elevation due to Nrf2 inhibition by ML385 aggravates the ferroptosis induced by RSL3.

Cells undergoing ferroptosis are usually marked by intracellular iron and lipid ROS accumulation. Later it became known that GPX4 is a crucial regulator of ferroptosis.[22] Hence, GPX4 inhibition, directly or indirectly, has been used to model ferroptosis.[23] In this study, we used a chemical inducer of ferroptosis, RSL3, to downregulate the expression of GPX4. Our data showed that beas-2b is relatively more sensitive to RSL3 compared to other types of cells such as cardiomyoblast,[24] renal epithelial cells,[25] and neuronal cells[26] as a minimal concentration (40 nM) of RSL3 can reduce cell viability up to 70%. This suggests the lung may be more prone to ferroptosis. Since Nrf2 is a crucial regulator of the antioxidant response, we used ML385 to inhibit Nrf2 with a concentration (0.5 μM) that has little effect on cell viability. Our data showed ML385 and RSL3 combination has synergism effect showed by CI value less than 1.[27] To our surprise, mitochondrial ROS is markedly elevated when ML385 is combined with RSL3. We suggest the excessive mitochondrial ROS triggered by ML385 plays a crucial role in the beas-2b ferroptosis. To confirm this, we employed Mito TEMPOL, a specific mitochondrial ROS scavenger.[28] Our data demonstrated that Mito TEMPOL application prevents mitochondrial ROS elevation and further reduction in cell viability. Furthermore, Mito TEMPOL application also restores the GPX4 expression comparable to the control group. Unexpectedly, Mito TEMPOL application could not restore the Nrf2 protein level to normal, indicating that the rescuing effect of Mito TEMPOL is independent of Nrf2.

Ferroptosis is also marked by intracellular iron accumulation. To facilitate this, Transferrin Receptor 1 (TfR1) is upregulated in ferroptosis cells, bringing ferritin into the cells.[29] Previous publications have revealed that TfR1 is a specific marker of ferroptosis.[19,20] In beas-2b cells, RSL3 with or without ML385 upregulates the expression of TfR1. Intriguingly, the Mito TEMPOL application prevents the upregulation of TfR1.

Lipid ROS upregulation is a characteristic of ferroptosis. Recent study has shown that mitochondrial lipid ROS also contributes to ferroptosis induced by RSL3.[30] To our surprise, our results revealed that Mito TEMPOL pretreatment restored the lipid ROS level back to normal. This shows the crucial role mitochondria play in protecting cells from lipid ROS. In addition, we also demonstrated that Mito TEMPOL rescued the reduction in the mitochondrial membrane potential induced by RSL3. However, the effects became less significant at higher concentrations of RSL3. To further clarify the role of mitochondrial function, we assessed the expression of the mitochondrial OXPHOS complex. Treatment with RSL3 with or without ML385 showed a lower expression pattern in complex II and IV. Mito TEMPOL treatment restored levels similar to the control. Complex II can be both a suppressor or enhancer of ROS[31] while complex IV main function is to reduce oxygen to water. Previous study further showed that the loss or inhibition of complex IV may lead to loss in complex II activity.[32] Thus, our results suggest that ML385 and RSL3 combination further impairs the mitochondrial respiratory chain and worsens ferroptosis by reducing complex II and complex IV.

Altogether, we showed that mitochondrial ROS and mitochondrial function plays a crucial role in ferroptosis. Therefore, targeting mitochondria and mitochondrial ROS holds promising strategies to combat ferroptosis-related diseases. Further studies in the animal and other type of cells are vital to reveal the more profound role of ferroptosis and mitochondrial ROS.

Author contributions

IPT and JHS conceived of the study, conducted the experiment, analyzed the data, and wrote the manuscript. RF, ST, SS, LYY, YTC, and CYH supervised the study. IPT, LYY, YTC, and CYH contributed reagents/materials/analysis tools. All authors reviewed and approved the final manuscript.

Declaration of conflicting interests

The author(s) declared no potential conflicts of interest with respect to the research, authorship, and/or publication of this article.

Funding

The author(s) disclosed receipt of the following financial support for the research, authorship, and/or publication of this article: This study was supported by Universitas Muhammadiyah Yogyakarta, Indonesia (Grant number: 01/RIS-LRUU2022), Buddhist Tzu Chi General Hospital (Grant number: IMAR-111-01–08) and by the Ministry of Science and Technology, Taiwan (Grant number: MOST 110-2314-B-303-006).

ORCID iDs

JH Situmorang https://orcid.org/0000-0003-3288-6814
C-Y Huang https://orcid.org/0000-0003-2347-0411

References

1. Dixon SJ and Stockwell BR. The role of iron and reactive oxygen species in cell death. *Nat Chem Biol* 2014; 10(1): 9–17.
2. Xu W, Deng H, Hu S, et al. Role of ferroptosis in lung diseases. *J Inflamm Res* 2021; 14: 2079–2090.

3. Yan HF, Zou T, Tuo Qz, et al. Ferroptosis: mechanisms and links with diseases. *Signal Transduct Target Ther* 2021; 6(1): 49.
4. Lei P, Bai T and Sun Y. Mechanisms of ferroptosis and relations with regulated cell death: a review. *Front Physiol* 2019; 10: 139.
5. Yang WS, SriRamaratnam R, Welsch M, et al. Regulation of ferroptotic cancer cell death by GPX4. *Cell* 2014; 156(1–2): 317–331.
6. Kerins MJ and Ooi A. The roles of NRF2 in modulating cellular iron homeostasis. *Antioxid Redox Signal* 2018; 29(17): 1756–1773.
7. Gan B. Mitochondrial regulation of ferroptosis. *J Cell Biol* 2021; 220(9): e202105043.
8. Singh A, Venkannagari S, Oh KH, et al. Small molecule inhibitor of NRF2 selectively intervenes therapeutic resistance in KEAP1-deficient NSCLC tumors. *ACS Chem Biol* 2016; 11(11): 3214–3225.
9. Kauffman ME, Kauffman MK, Traore K, et al. MitoSOX-based flow cytometry for detecting mitochondrial ROS. *React Oxyg Species (Apex)* 2016; 2(5): 361–370.
10. Roelofs BA, Ge SX, Studlack PE, et al. Low micromolar concentrations of the superoxide probe MitoSOX uncouple neural mitochondria and inhibit complex IV. *Free Radic Biol Med* 2015; 86: 250–258.
11. Martinez AM, Kim A and Yang WS. Detection of ferroptosis by BODIPY 581/591 C11. *Methods Mol Biol* 2020; 2108: 125–130.
12. Sivandzade F, Bhalerao A and Cucullo L. Analysis of the mitochondrial membrane potential using the cationic JC-1 dye as a sensitive fluorescent probe. *Bio Protoc* 2019; 9(1): e3128.
13. Lin YM, Situmorang JH, Guan JZ, et al. ZAKbeta alleviates oxidized low-density lipoprotein (ox-LDL)-induced apoptosis and B-type natriuretic peptide (BNP) upregulation in cardiomyoblast. *Cell Biochem Biophys* 2022; 80(3): 547–554.
14. Yang CM, Yang C-C, Hsiao LD, et al. Upregulation of COX-2 and PGE2 induced by TNF-alpha mediated through TNFR1/MitoROS/PKCalpha/P38 MAPK, JNK1/2/FoxO1 cascade in human cardiac fibroblasts. *J Inflamm Res* 2021; 14: 2807–2824.
15. Im K, Mareninov S, Diaz MFP, et al. An introduction to performing immunofluorescence staining. *Methods Mol Biol* 2019; 1897: 299–311.
16. Dodson M, Castro-Portuguez R and Zhang DD. NRF2 plays a critical role in mitigating lipid peroxidation and ferroptosis. *Redox Biol* 2019; 23: 101107.
17. Seibt TM, Proneth B and Conrad M. Role of GPX4 in ferroptosis and its pharmacological implication. *Free Radic Biol Med* 2019; 133: 144–152.
18. Dachert J, Schoeneberger H, Rohde K, et al. RSL3 and Erastin differentially regulate redox signaling to promote Smac mimetic-induced cell death. *Oncotarget* 2016; 7(39): 63779–63792.
19. Feng H, Schorpp K, Jin J, et al. Transferrin receptor is a specific ferroptosis marker. *Cell Rep* 2020; 30(10): 3411–3423 e7.
20. Jin J, Schorpp K, Samaga D, et al. Machine learning classifies ferroptosis and apoptosis cell death modalities with TfR1 immunostaining. *ACS Chem Biol* 2022; 17(3): 654–660.
21. Li J, Cao F, Yin Hl, et al. Ferroptosis: past, present and future. *Cell Death Dis* 2020; 11(2): 88.
22. Friedmann Angeli JP, Schneider M, Proneth B, et al. Inactivation of the ferroptosis regulator Gpx4 triggers acute renal failure in mice. *Nat Cell Biol* 2014; 16(12): 1180–1191.
23. Conrad M and Friedmann Angeli JP. Glutathione peroxidase 4 (Gpx4) and ferroptosis: what's so special about it? *Mol Cell Oncol* 2015; 2(3): e995047.
24. Park TJ, Park JH, Lee GS, et al. Quantitative proteomic analyses reveal that GPX4 downregulation during myocardial infarction contributes to ferroptosis in cardiomyocytes. *Cell Death Dis* 2019; 10(11): 835.
25. Adedoyin O, Boddu R, Traylor A, et al. Heme oxygenase-1 mitigates ferroptosis in renal proximal tubule cells. *Am J Physiol Renal Physiol* 2018; 314(5): F702–F714.
26. Li M, Song D, Chen X, et al. RSL3 triggers glioma stem cell differentiation via the Tgm2/AKT/ID1 signaling axis. *Biochim Biophys Acta Mol Basis Dis* 2022; 1868(12): 166529.
27. Zhao L, Au JL and Wientjes MG. Comparison of methods for evaluating drug-drug interaction. *Front Biosci (Elite Ed)* 2010; 2(1): 241–249.
28. Trnka J, Blaikie FH, Logan A, et al. Antioxidant properties of MitoTEMPOL and its hydroxylamine. *Free Radic Res* 2009; 43(1): 4–12.
29. Li L, Fang CJ, Ryan JC, et al. Binding and uptake of H-ferritin are mediated by human transferrin receptor-1. *Proc Natl Acad Sci U S A* 2010; 107(8): 3505–3510.
30. Wu S, Mao C, Kondiparthi L, et al. A ferroptosis defense mechanism mediated by glycerol-3-phosphate dehydrogenase 2 in mitochondria. *Proc Natl Acad Sci U S A* 2022; 119(26): e2121987119.
31. Drose S. Differential effects of complex II on mitochondrial ROS production and their relation to cardioprotective pre- and post-conditioning. *Biochim Biophys Acta* 2013; 1827(5): 578–587.
32. Hargreaves IP, Duncan A, Wu L, et al. Inhibition of mitochondrial complex IV leads to secondary loss complex II-III activity: implications for the pathogenesis and treatment of mitochondrial encephalomyopathies. *Mitochondrion* 2007; 7(4): 284–287.